PHYSICAL REVIEW C **73**, 044324 (2006)

α-decay of the new isotope ^{187}Po: Probing prolate structures beyond the neutron mid-shell at N = 104

A. N. Andreyev,[1,7] S. Antalic,[2] D. Ackermann,[3,8] S. Franchoo,[4] F. P. Heßberger,[3] S. Hofmann,[3,9] M. Huyse,[5] I. Kojouharov,[3] B. Kindler,[3] P. Kuusiniemi,[3] S. R. Lesher,[5] B. Lommel,[3] R. Mann,[3] G. Münzenberg,[3,8] K. Nishio,[3,10] R. D. Page,[6] J. J. Ressler,[7] B. Streicher,[2] S. Saro,[2] B. Sulignano,[3] P. Van Duppen,[5] D. Wiseman,[6] and R. Wyss[11]

[1] *TRIUMF, 4004 Wesbrook Mall, Vancouver, British Columbia, Canada V6T 2A3*
[2] *Department of Nuclear Physics and Biophysics, Comenius University, Bratislava SK-84248, Slovakia*
[3] *Gesellschaft für Schwerionenforschung, Planckstrasse 1, D-64291 Darmstadt, Germany*
[4] *IPN Orsay, F-91406 Orsay Cedex, France*
[5] *Instituut voor Kern- en Stralingsfysica, K.U. Leuven, University of Leuven, B-3001 Leuven, Belgium*
[6] *Department of Physics, Oliver Lodge Laboratory, University of Liverpool, Liverpool L69 7ZE, United Kingdom*
[7] *Department of Chemistry, Simon Fraser University, Burnaby, British Columbia, Canada V5A-1S6*
[8] *Institut fur Physik, Johannes Gutenberg-University, D-55099 Mainz, Germany*
[9] *Physikalisches Institut, J.W. Goethe-Universität, D-60054 Frankfurt, Germany*
[10] *Advanced Science Research Center, Japan Atomic Energy Agency, Tokai, Ibaraki 319-1195, Japan*
[11] *Department of Physics, Royal Institute of Technology, 104 05 Stockholm, Sweden*

(Received 7 February 2006; published 25 April 2006)

The new neutron-deficient isotope ^{187}Po has been identified in the complete fusion reaction ^{46}Ti+^{144}Sm $\rightarrow$ ^{187}Po+3n at the velocity filter SHIP. Striking features of the ^{187}Po α decay are the strongly-hindered decay to the spherical ground state and unhindered decay to a surprisingly low-lying deformed excited state at 286 keV in the daughter nucleus ^{183}Pb. Based on the potential energy surface calculations, the ^{187}Po ground state and the 286 keV excited state in ^{183}Pb were interpreted as being of prolate origin. The systematic deviation of the α-decay properties in the lightest odd-A Po isotopes relative to the smooth behavior in the even-A neighbors is discussed. Improved data for the decay of ^{187}Bi^{m,g} were also obtained.

DOI: 10.1103/PhysRevC.73.044324 PACS number(s): 23.60.+e, 27.70.+q

I. INTRODUCTION

In the neutron-deficient Po isotopes the richest examples of shape coexistence at low excitation energy can be found. Historically, the first work in which shape coexistence in these nuclei was discussed was the Nilsson-Strutinsky calculations by May *et al*. [1]. The authors suggested a gradual change of the Po ground state (g.s.) from a nearly spherical configuration around the neutron shell closure at $N = 126$ (^{210}Po), to an oblate configuration in the vicinity of ^{192}Po, with a prolate ground state expected close to and beyond the neutron mid-shell at $N = 104$ (^{188}Po). It is important to stress that practically all modern approaches, based both on improved Nilsson-Strutinsky methods or on self-consistent Hartree-Fock-Bogoliubov calculations, are in agreement with the earlier study by May *et al*., see discussion, e.g., in Refs. [2,3].

These theoretical findings are strongly supported by complementary data both from in-beam studies, see, e.g., Refs. [4,5] and particle (β and α) decay (e.g., Refs. [6–12]), which provided extensive systematics on the evolution of shape coexistence in the long sequence of $^{188-210}$Po isotopes. However, due to low production cross sections and high background from fission, the most neutron-deficient Po nuclei cannot presently be investigated with in-beam techniques, ^{190}Po being the lightest Po isotope studied by this method so far [5,13] (the current cross section limit for this technique is $\sigma \sim 50$ nb).

On the other hand, α decay has proven to be a sensitive tool to study shape coexistence in nuclei, providing information on both parent and daughter states involved in the decay, see, e.g., Refs. [14,15]. Furthermore, nuclei with production cross sections in the subnanobarn region become accessible. A recent example of such work is our α-decay study of the neutron-deficient isotopes ^{188,189}Po (see Ref. [12] and references therein), which are presently not accessible by any other methods.

A striking observation in the ^{189}Po α decay was that the 7532 keV g.s.$\rightarrow$g.s. α decay to the spherical ground state in the daughter isotope ^{185}Pb was hindered by a factor of $\sim$77 (in terms of reduced α widths as defined by Rasmussen [16]) relative to the 7259 keV fine structure (f.s.) α decay to an excited state at 278 keV in ^{185}Pb [12]. A similar pattern, though with a lower hindrance factor (HF) of $\sim$12 for the 7910 keV g.s.$\rightarrow$g.s. decay relative to the 7355 keV fine structure α decay was also observed in the neighboring isotope ^{188}Po [11]. Combined with the potential energy surface calculations, these data provided the first experimental evidence that the ground states of ^{188,189}Po and the excited states in their respective daughters ^{184,185}Pb, fed by unhindered fine structure decays, are of prolate origin, see details in Refs. [11,12]. The sphericity of the ground states in the isotopes ^{184,185}Pb was recently proved by the charge radii measurements [17].

The present study extends our previous work in this region, performed at the velocity filter SHIP of the GSI in Darmstadt [18,19] and reports on an α-decay study of the new isotope ^{187}Po. The data for the new isotopes ^{186}Po and ^{192}At, identified in the same experiment, will be discussed elsewhere [20,21].

II. EXPERIMENTAL SET-UP

A detailed discussion of the experimental method was given in our recent paper, which dealt with the identification of a new isotope ^{192}At [20] performed in the same experiment (by using the ^{51}V beam). Therefore, only a short description of the experimental procedure will be given here.

The nucleus ^{187}Po was produced in the ^{144}Sm(^{46}Ti,3n)^{187}Po complete fusion reaction. A pulsed ^{46}Ti beam (5 ms on/15 ms off) with an intensity of ~200 pnA was provided by the UNILAC heavy ion accelerator of the GSI. The measurements were performed at six beam energies in the range of 202–242 MeV in the middle of the target to estimate the maxima of the excitation functions for different evaporation channels. The data for ^{187}Po were collected at the energy of $E(^{46}\mathrm{Ti}) =$ 224(1) MeV in front of the target. Eight 400 μg/cm^2 thick ^{144}Sm targets were mounted on a target wheel, rotating synchronously with the UNILAC macro-pulsing. The targets were produced by evaporating ^{144}SmF$_3$ material (96.47% enriched) onto a carbon backing of 40 μg/cm^2 thickness and covered with a 10 μg/cm^2 carbon layer to increase the radiative cooling and reduce the sputtering of the material.

After separation by the velocity filter SHIP [18] the recoiling evaporation residues were implanted into a 300 μm thick, 35×80 mm^2 16-strip position-sensitive silicon detector (PSSD), where their subsequent particle decays were measured [19].

The usual detection system consisting of six silicon BOX detectors, three time-of-flight detectors [22] and a "veto" detector, which are described in detail in Refs. [20,23] was used. The time-of-flight detectors (TOF) installed in front of the BOX+PSSD system allowed us to distinguish the reaction products from the scattered beam particles. More importantly, decay events in the PSSD could be distinguished from the implantation events by requiring an anticoincidence condition between the signals from the PSSD and from at least one of the TOF detectors.

A large-volume four-fold segmented Clover-type germanium detector was installed behind the PSSD for the recoil-γ and/or α-γ [ΔT(particle-γ) $\leqslant$ 5 μs] coincidence measurements. The absolute efficiency calibration for this detector is described in Ref. [24].

III. EXPERIMENTAL RESULTS

A. α decay of ^{187}Po

Figure 1(a) shows a part of the α spectrum measured in the PSSD in anticoincidence with the signals from the TOF and veto detectors. The peaks at 6699(5) keV [^{195m}Po [25], not shown in Fig. 1(a)], at 6842(6) keV (^{194}Po [25]) and at 7612(15) keV (^{187}Bi^g [26]) were used for α-energy calibration in this energy region. As shown below, three nuclides contribute to the peak at $E_\alpha = 7000(20)$ keV: ^{193}Po^m ($E_\alpha = 7004(5)$ keV [25]), ^{188}Bi^{m2} ($E_\alpha = 6992(5)$ keV [27]) and ^{187}Bi^g ($E_\alpha = 7000(8)$ keV [26]). The A(Po) $\geqslant$ 190 isotopes were produced in reactions on the admixtures of the heavier Sm isotopes in the target, while the ^{187,188}Bi isotopes were produced in the p,2n and p,1n channels of the studied reaction, respectively. Figure 1(b) shows the same spectrum as in Fig. 1(a), but registered within the time interval of ΔT(recoil-α_1) $\leqslant$ 7 ms after the recoil implantation, which clearly enhances the α peaks from the short-lived activities (e.g., ^{187}Bi^m).

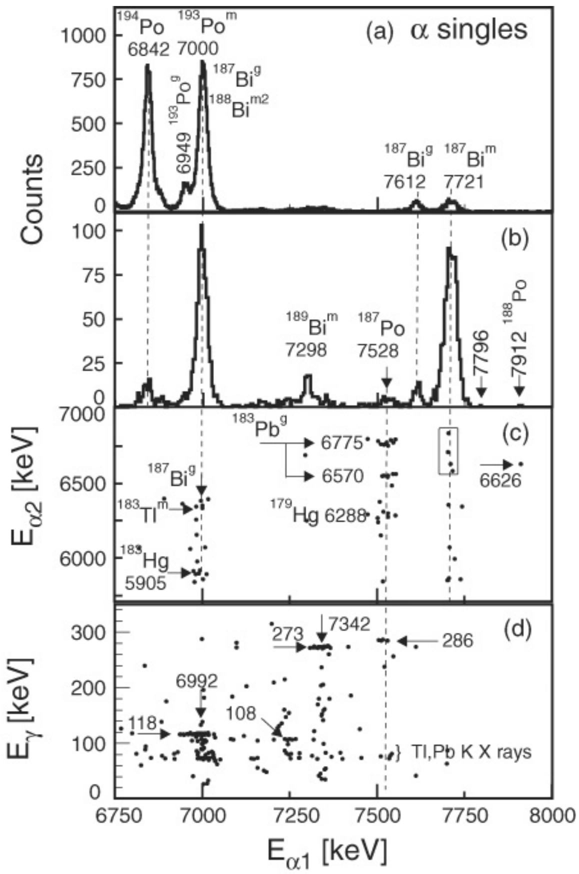

FIG. 1. (a) A part of the α_1-energy spectrum from the reaction ^{46}Ti(224 MeV)+^{144}Sm $\rightarrow$ ^{190}Po* registered in the whole PSSD. (b) The same spectrum as in (a), but registered within the time interval ΔT(recoil-α_1) $\leqslant$ 7 ms after the recoil implantation; (c) the two-dimensional $E_{\alpha1}$-$E_{\alpha2}$ plot for ΔT(recoil-α_1) $\leqslant$ 7 ms and ΔT(α_1-α_2) $\leqslant$ 3 s. The open rectangle is explained in the text; (d) $E_{\alpha1}$-E_γ spectrum for α_1 events in coincidence with γ rays, ΔT(recoil-α_1) $\leqslant$ 100 ms and ΔT(α_1-γ) $\leqslant$ 5 μs. α- and γ-decay energies are given in keV.

Figure 1(c) shows the result of the recoil-α_1-α_2 time-position correlation analysis for the time intervals of ΔT(recoil-α_1) $\leqslant$ 7 ms and $\Delta T(\alpha_1 - \alpha_2) \leqslant$ 3 s.

The α decay at $E_\alpha = 7528(15)$ keV in Fig. 1(b) and 1(c) is attributed to the new isotope ^{187}Po as it clearly correlates with both known α decays of the $I^\pi = 3/2^-$ ground state of the daughter isotope ^{183}Pb ($T_{1/2} = 535(30)$ ms, $E_\alpha =$ 6570(10) keV, $I_\alpha = 28(4)\%$ and $E_\alpha = 6775(7)$ keV, $I_\alpha =$ 72(5)% [28], see Fig. 2). Furthermore, it also correlates with the α decay of the grand-daughter nucleus ^{179}Hg ($E_\alpha =$ 6288(5) keV, $T_{1/2} = 1.09$ s [29]). The good match of the measured decay properties with the literature data for the daughter isotopes proves that the parent decay at 7528 keV originates from ^{187}Po. A half-life value of $T_{1/2} = 1.40(25)$ ms was deduced for ^{187}Po.

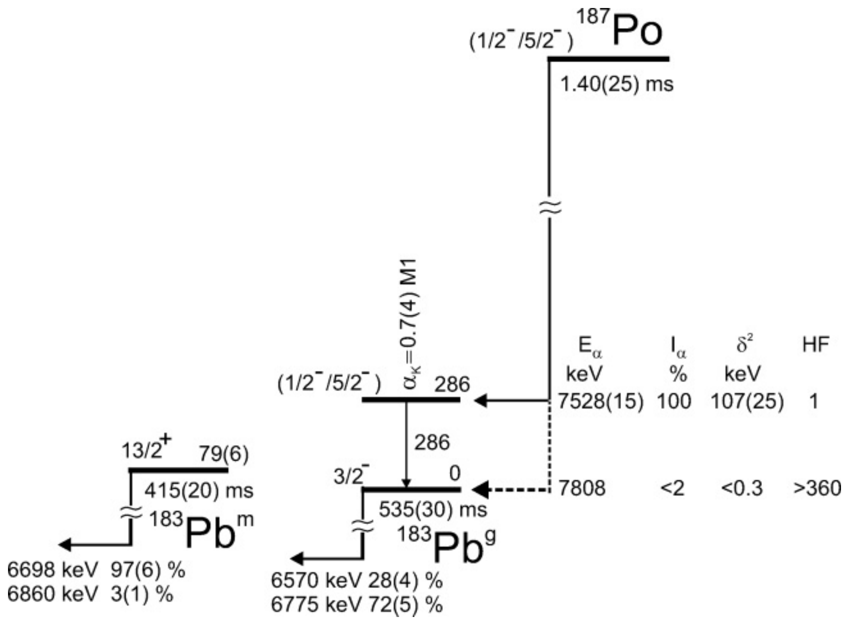

FIG. 2. Decay scheme of ^{187}Po deduced in this work. Shown are α-decay energies E_α, intensities I_α, reduced α widths δ_α^2 and hindrance factor values HF. The tentative 7808 keV decay is shown by the dashed line. The I^π assignments in ^{187}Po and of the 286 keV state in ^{183}Pb are tentative and based on a combination of the PES/PPR calculations and α decay hindrance factors, see text for details. Note that both $I^\pi = 1/2^-$ or $5/2^-$ are possible for ^{187}Po and for the 286 keV state in ^{183}Pb, but the I^π assignments must be the same for both states. The I^π values for both α-decaying states in ^{183}Pb were deduced in [17]. The decay scheme of ^{183}Pb was taken from [28].

A few other groups of correlated decays in Fig. 1(c) are readily understood as due to the decay of other known nuclei. Two groups of correlated events starting from the $E_{\alpha 1} = 7000$ decay are due to correlation of ^{187}Bi^g with the complex α decay of its daughter ^{183}Tl^m (three α lines in the region of 6333–6456 [30], see Fig. 3) and with the 5905 keV α decay of its grand-daughter ^{183}Hg (after β decay of ^{183}Tl). A single correlated recoil-α_1(7912 keV)-α_2(6626 keV) event is due to the decay of ^{188}Po [11]. Note that two events at 7912(15) keV are also present in the recoil-α_1 spectrum in Fig. 1(b), one of them is the same as in Fig. 1(c). The events seen in correlations with the 7720 keV decay will be discussed in the next section.

Figure 1(d) shows the plot of recoil-[α_1-γ] events for the time intervals of ΔT(recoil-α_1) $\leqslant 100$ ms and $\Delta T(\alpha_1$-$\gamma) \leqslant 5\mu$s. Though the former time interval is not optimal for the decay of ^{187}Po, it was chosen to include the events from the decay of ^{187}Bi^g [$T_{1/2} = 40(2)$ ms, see discussion below]. The group of coincident α_1(6992 keV)-γ(118 keV) events originates from the known decay of ^{188}Bi^{m2} [27], while the α_1(7260 keV)-γ(108 keV) group is due to the decay of ^{186}Bi [31].

Figure 1(d) shows that the 7528 keV decay of ^{187}Po is in coincidence with the 286(1) keV γ decay (five events) and with the Pb K-x rays. This identifies an excited state at 286 keV above the $3/2^-$ ground state in ^{183}Pb. From the ratio of the number of full energy 286 keV decays and Pb K-x rays in coincidence with the 7528 keV decay, the K-shell conversion coefficient of $\alpha_K = 0.7(4)$ was deduced. This tentatively establishes $M1$ multipolarity for the 286 keV transition as the calculated conversion coefficients are [32]: $\alpha_K(E1) = 0.027$, $\alpha_K(E2) = 0.073$, $\alpha_K(M1) = 0.42$, $\alpha_K(M2) = 1.46$.

Based on the full Q_α-value analysis [$Q_{\alpha,\text{full}} = Q_\alpha$(7528 keV)$+E_\gamma$(286 keV)], a full-energy crossover transition with the energy of $E_\alpha = 7808(15)$ keV feeding directly to the $3/2^-$ ground state of ^{183}Pb could be expected. A single α decay at 7796(15) keV in Fig. 1(b) which occurred 1.1 ms after the recoil implantation could be considered as a candidate for this crossover transition. Using this single event as an upper limit for the intensity of the tentative crossover transition, the decay scheme of ^{187}Po was constructed as shown in Fig. 2. The discussion of spin-parity for the newly identified states will be given in the following sections.

A comment on four recoil-α_1(7720(20) keV)-α_2(6600–6800 keV) correlated events, marked by the rectangle in Fig. 1(c), should be made here. The energy and half-life values of the α_2 decays are in agreement with the decay properties

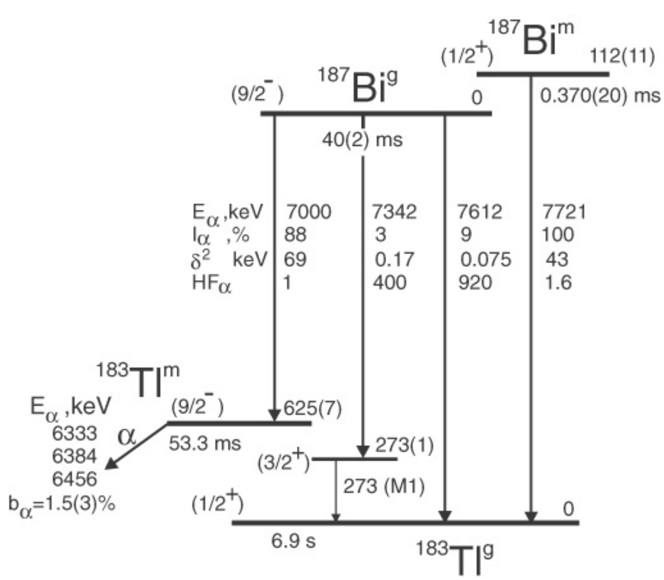

FIG. 3. Decay scheme of ^{187}Bi deduced in this work. Shown are α-decay energies E_α, relative intensities I_α, reduced α widths δ_α^2 and hindrance factor values HF. The HF values were calculated relative to the unhindered 7000 keV decay of ^{187}Bi^g, for which HF = 1 was assumed. All I^π assignments are tentative and shown in brackets. The data for ^{183}Tl are taken from Refs. [29,30], except for the α-branching ratio of $b_\alpha(^{183}\text{Tl}^m) = 1.5(3)\%$ and position of the excited state at $E^* = 273(1)$ keV measured in our study.

of both isomeric states in ^{183}Pb, see Fig. 2, thus the parent α_1 decays must originate from ^{187}Po. One of the sources for these events could the energy summing in the PSSD of the 7528 keV decay and Pb K-shell conversion electrons from the subsequent 286 keV transitions, which gives the full-energy peak at ∼7726 keV. On the other hand, the 7720(20) keV decay could be the decay of a second α-decaying state in ^{187}Po ($T_{1/2} \sim 0.5$ ms).

However, the low number of correlated events prevents us from drawing a firm conclusion on the nature of observed recoil-α_1(7720(20) keV)-α_2(6600–6800 keV) correlated events.

B. α decay of ^{187}Bi

The previous α-decay data for ^{187}Bi^{m,g} come mainly from the study in Ref. [26]. However, only a relatively low number of counts was observed for some of the α decays, e.g., $\leqslant 15$ events for the 7612 keV decay of ^{187}Bi^g and for the 7721 keV decay of ^{187}Bi^m (see Fig. 1 of Ref. [26]). Due to this, some assignments were tentative and no experimental uncertainties were given for the relative intensities of different α lines (see Table I).

In the present experiment, we collected a number of ^{187}Bi^{m,g} α decays at least one order of magnitude larger than in any of the three earlier studies of this nucleus [26,33,34]. This resulted in improved α-decay data for both isomeric states in this nucleus, see Fig. 3 and Table I.

Due to some contamination from ^{193}Po^m [$E_\alpha =$ 7004(5) keV] and ^{188}Bi^{m2} [$E_\alpha = 6992(5)$ keV], the strongest α decay of ^{187}Bi^g at 7000 keV was not used in our study for improved half-life determination of this nucleus. Instead, the second strongest decay of ^{187}Bi^g at 7612(5) keV (relative intensity $I_{\alpha,\mathrm{rel}} = 9\%$, Fig. 3) was used with ∼750 correlated events obtained for the ΔT[recoil-α_1(7612 keV)] $\leqslant 500$ ms time interval. For comparison, this value is still ∼10 times larger than the number of counts in the main 7000 keV peak of ^{187}Bi^g in Fig. 1 of Ref. [26]. The deduced half-life value of $T_{1/2} = 40(2)$ ms for ^{187}Bi^g is consistent with but more precise than any of the three previously reported values of $T_{1/2} =$ 32(3) ms [26], $T_{1/2} = 45(11)$ ms [33] and $T_{1/2} = 35^{+14}_{-8}$ ms [34].

A half-life value of $T_{1/2} = 370(20)$ μs was deduced for the 7721(10) keV α decay of ^{187}Bi^m [∼950 recoil-α(7721 keV) events]. This is a more precise value in comparison with two earlier measurements of $T_{1/2} = 290^{+90}_{-50}$ μs [26] and $T_{1/2} = 310^{+190}_{-90}$ μs [34], both based on a handful of observed events only.

The improved energy precision for the 7612(5) keV and 7000(5) keV transitions establishes a more precise value of 625(7) keV for the excitation energy of the 9/2$^-$ intruder state in ^{183}Tl (the previous value was 625(17) keV [26]). Similarly, the 7721(10) and 7612(5) keV decays provide a more precise value of 112(11) keV for the excitation energy of the 1/2$^+$ intruder state in ^{187}Bi relative to the 9/2$^-$ ground state (the previous value was 112(21) keV [26]).

The group of 19 α_1(7342(15) keV)-γ(273(1) keV) events in Fig. 1(d) has a full Q_α-value that is in good agreement with the Q_α-value for the 7612 keV decay of ^{187}Bi^g. The measured half-life of $T_{1/2} = 40(10)$ ms for the 7342 keV decay agrees well with the half-life of ^{187}Bi^g. On these grounds the 7342 keV decay was assigned as proceeding from the 9/2$^-$ ground state of ^{187}Bi toward presumably the 3/2$^+$ state at 273 keV in the daughter nuclide ^{183}Tl, which further deexcites to the 1/2$^+$ ground state in this nucleus. Based on the ratio of the number of the full energy 273 keV decays and Tl K-x rays in coincidence with the 7342 keV decay, a K-shell conversion coefficient of $\alpha_K = 0.55(15)$ was deduced. From the comparison with the calculated values of α_K for the $M1$, $M2$, $E1$, $E2$ multipolarities taken from Ref. [32], the experimental value suggests an $M1$ multipolarity for the 273 keV transition, supporting the $I^\pi = 3/2^+$ assignment for the 273 keV excited state in ^{183}Tl. Thus, our data provide the direct measurement for the excitation energy of the 3/2$^+$ in ^{183}Tl as $E^* = 273(1)$ keV. This is a more precise value in comparison with $E^* = 250(34)$ keV deduced in Ref. [26], in which no γ-decay measurements were performed and the excitation energy was deduced from a few 7367(30) keV α decays tentatively assigned as the $9/2^- \rightarrow 3/2^+$ transition of ^{187}Bi^g. The absolute intensity of the 7342 keV line was calculated based on the number of recoil-[α_1(7342)-γ(273 keV)] coincidences in Fig. 1(d), normalized on the corresponding γ-ray efficiency and conversion coefficient of the 273 keV γ ray.

To deduce the relative intensities of the 7000(5), 7342(15) and 7612(5) keV lines of ^{187}Bi^g we had to estimate the contributions of ^{193}Po^m ($E_\alpha = 7004$ keV) and of

TABLE I. Our measured decay data for ^{187}Bi together with the earlier data from Ref. [26]. Shown are isomer assignments, α-decay energies E_α, relative intensities I_α, reduced α widths δ^2_α, hindrance factors HF. The reduced α widths were calculated with the Rasmussen prescription [16] by assuming $\Delta L = 0$ decays. The HF values were calculated relative to the unhindered $(9/2^-) \rightarrow (9/2^-)$ decay of ^{187}Bi^g, for which HF = 1 was assumed. All I^π assignments are tentative and shown in brackets. Note that no experimental errors were given in Ref. [26] for the relative intensities of different α lines in ^{187}Bi^g.

	Our data						Literature data, [26]		
Isomer, I^π	$T_{1/2}$ [ms]	E_α [keV]	I_α [%]	$I_i \rightarrow I_f$	δ^2_α [keV]	HF	$T_{1/2}$ [ms]	E_α [keV]	I_α [%]
^{187}Bi^g, $(9/2^-)$	40(2)	7000(5)	88(4)	$(9/2^-) \rightarrow (9/2^-)$	69(4)	1	32(3)	7000(8)	88.3
		7342(15)	3.0(7)	$(9/2^-) \rightarrow (3/2^+)$	0.17(4)	400(100)		7367(30)	3.7
		7612(5)	9.0(5)	$(9/2^-) \rightarrow (1/2^+)$	0.075(5)	920(70)		7612(15)	8.0
^{187}Bi^m, $(1/2^+)$	0.370(20)	7721(10)	100	$(1/2^+) \rightarrow (1/2^+)$	43(3)	1.60(16)	$0.29^{+0.09}_{-0.05}$	7721(15)	100

^{188}Bi^{m2} ($E_\alpha = 6992$ keV) to the 7000(20) keV peak in Fig. 1(a). The contribution of ^{188}Bi was deduced based on the number of α_1(6992)-γ(118 keV) coincidences [c.f. Fig. 1(d)], normalized on the corresponding γ-ray efficiency and conversion coefficient of the 118 keV γ ray. The absolute amount of ^{193}Po^m in the 7000 keV line was estimated by using the intensity of ^{193}Po^g ($E_\alpha = 6949$ keV [25]) and the typical isomeric ratio, observed in complete-fusion reactions, of $I(^{193}\text{Po}^m)/I(^{193}\text{Po}^g)\sim 2.0(2)$ (see, e.g., Fig. 1 of Ref. [11]).

Finally, the relative intensities of the three lines were deduced, which allowed us to calculated the reduced α widths δ_α^2 and hindrance factor values as shown in Fig. 3 and Table I. The HF values were calculated relative to the $9/2^- \rightarrow 9/2^-$ 7000 keV decay of ^{187}Bi^g. This decay (and similar decays in the odd-A Bi isotopes) represents a good example of unhindered α decay in this mass region, as it connects two identical single particle configurations in the parent and daughter nuclei, see Ref. [35] and references therein.

An isomeric ratio of $I(^{187}\text{Bi}^g)/I(^{187}\text{Bi}^m) = 7.0(2)$ was determined, which follows the trend of the preferential population in the complete-fusion reactions of the $9/2^-$ ground state relative to the $1/2^+$ isomeric state, observed in the heavier odd-A α-decaying Bi isotopes. In this respect, the sudden change to the preferential population of the $1/2^+$ state in ^{185}Bi along with the nonobservation of the $9/2^-$ state in this nucleus is not yet understood, see also discussion in Ref. [35].

C. α-branching ratio of ^{183}Tl^m

The α-branching ratio for ^{183}Tl^m was deduced by using the mother-daughter intensity relations and comparing the number of the $E_{\alpha_1} = 7000$ keV decays of ^{187}Bi^g in the singles α spectrum in Fig. 1(a) and the number of α_1 (7000 keV)-α_2(6300–6500 keV, ^{183}Tl^m) correlated events for the time $\Delta T(\alpha_1\text{-}\alpha_2) \leqslant 200$ ms. The former number was corrected for the contribution of ^{193}Po^m and ^{188}Bi as described above. The correlation time interval was chosen equal to four half-lives of ^{183}Tl^m ($T_{1/2}(^{183}\text{Tl}^m) = 53.3(3)$ ms [30]) to specifically enhance the ^{187}Bi^g-^{183}Tl^m correlations. The resulting value of $b_\alpha(^{183}\text{Tl}^m) = 1.5(3)\%$ is in agreement with the two previously measured values of $\sim$1.5% (one observed correlated event only) [26] and $\sim$2% from Ref. [30]. Note that no experimental errors were given for b_α in both studies [26,30].

No α- or β-branching ratio estimate was possible for ^{183}Tl^g in our study.

D. Production cross sections of ^{187}Po and ^{187}Bi

The cross-section values of $\sigma(^{187}\text{Po}) = 0.8(3)$ nb and $\sigma(^{187}\text{Bi}) = 200(80)$ nb were deduced at the beam energy of 224 MeV in front of the target [$\sim$220(1) MeV in the middle of the target], which corresponds to the measured maximum of the excitation function for ^{187}Bi and thus, for ^{187}Po. The data follow the systematical trend of the Po and Bi cross sections discussed in our recent study [36].

IV. DISCUSSION

A. Configurations and I^π assignments in ^{187}Po and ^{183}Pb

To understand the possible configurations of the new isotope ^{187}Po and of the 286 keV excited state in ^{183}Pb we performed potential energy surface (PES) and particle-plus-rotor (PPR) calculations for both nuclei. Such calculations were quite successful in describing the shape coexistence in the lead region, see our recent studies of $^{188-197}$Po and $^{184-193}$Pb isotopes [7–12]. In particular, we refer the reader to the studies [9,10], in which all the necessary details on these calculations were provided.

The potential energy surfaces for the negative parity states in ^{187}Po and ^{183}Pb are shown in Fig. 4(a) and 4(b), respectively. In ^{187}Po a prolate deformed minimum at $\beta_2 \sim 0.3$ is predicted to be the lowest in energy. In the daughter nucleus ^{183}Pb a spherical minimum coexists with a relatively low-lying prolate-deformed minimum at $\beta_2 \sim 0.27$ at a predicted energy of $E^* = 350$ keV only, which compares well with the experimental excitation energy of the 286 keV state in ^{183}Pb. The sphericity of the ground state in ^{183}Pb and its $I^\pi = 3/2^-$ assignment were recently proven by charge radii measurements [17]. From the PES calculations, in both ^{187}Po and ^{183}Pb, there is practically no evidence for oblate minima, thus the oblate configurations are not expected to play any role in our discussion. These conclusions are in agreement with the

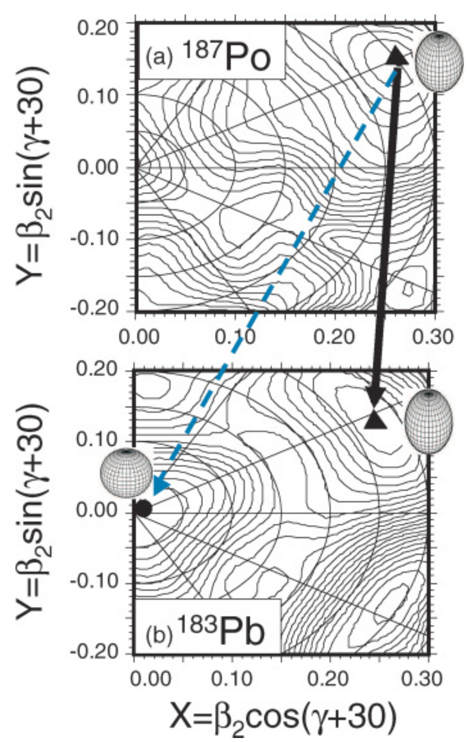

FIG. 4. (Color online) Potential energy surfaces for the negative parity states in ^{187}Po (a) and in ^{183}Pb (b). Spherical and prolate minima are indicated by respective shapes and solid circle and triangles, respectively. The solid arrow indicates the observed unhindered decay between two prolate configurations, while the dashed line corresponds to strongly hindered tentative decay to the spherical ground state of ^{183}Pb. The energy separation between the contour lines is 100 keV.

general trend in the lead region that the oblate configuration increases in energy beyond the neutron mid-shell at N = 104, while the prolate minimum appears to minimize its excitation energy around N = 100–104, see, e.g., Refs. [4,37,38].

Based on the PES calculations, the g.s. of ^{187}Po and the excited state at 286 keV in ^{183}Pb are assigned as prolate configurations. The PPR calculations suggest two close-lying negative-parity configurations in these nuclei: the 5/2$^-$[512] Nilsson state of mixed $2f_{7/2}$-$1h_{9/2}$ origin and the 1/2$^-$[521] state from the $2f_{5/2}$ orbital. Their close proximity in the calculations is due to the fact that for the neutron numbers of N = 101,103 the corresponding single particle orbitals cross at a prolate deformation of β_2 ~0.24, which is similar to the deformations predicted for the prolate minima in ^{183}Pb and ^{187}Po. This theoretical conclusion is confirmed by the well-established systematics of the lowest excited states in the isotone chains with N = 101 and N = 103. For example, all prolate-deformed N = 101 odd-*A* isotones of ^{183}Pb (^{169}Er, ^{171}Yb, ^{173}Hf, ^{175}W, ^{177}Os, ^{179}Pt, and ^{181}Hg) have the 1/2$^-$[521] ground state with a close-lying excited 5/2$^-$[512] state within 100–150 keV (where known) [29]. It is instructive to mention, that both $I^\pi = 5/2^-$ and $1/2^-$ assignments would be possible for the 286 keV state in ^{183}Pb based on the $I^\pi = 3/2^-$ assignment for the ground state of ^{183}Pb [17] and the $M1$ multipolarity of the 286 keV transition.

Similarly, in the prolate-deformed N = 103 isotones of ^{187}Po, some nuclei have a 5/2$^-$[512] g.s. state (e.g., ^{171}Er, ^{173}Yb, and ^{175}Hf), while others have the 1/2$^-$[521] ground state (e.g., ^{177}W, ^{179}Os, ^{181}Pt, and ^{183}Hg), with both configurations lying quite close in energy [29].

To summarize, both theoretical calculations and experimental systematics strongly point toward the $I^\pi = 1/2^-$ or 5/2$^-$ assignments for the g.s. of ^{187}Po and for the 286 keV excited state in ^{183}Pb. The actual I^π values will however depend on specific details for each isotope and are difficult to establish based on the above data alone.

Therefore, we used the ^{187}Po $\rightarrow$ ^{183}Pb α-decay pattern to shed more light on the I^π assignments in both isotopes. It is well known that unhindered α decay connects states of same spin, parity and configuration, while the decays connecting different Nilsson configurations are strongly hindered. As a relevant example we quote the case of the α decay of ^{181}Hg (N = 101), in which the 1/2$^-$[521] $\rightarrow$ 1/2$^-$[521] α decay is unhindered ($HF_\alpha = 0.6$), while the 1/2$^-$[521] $\rightarrow$ 5/2$^-$[512] α decay is hindered by a factor of $HF_\alpha = 422$ [29].

The 7258 keV decay of ^{187}Po feeding to the 286 keV state in ^{183}Pb can be considered as unhindered as its reduced α width is comparable with (in fact ~1.5 times larger than) the reduced α width of the unhindered 9/2$^-$ $\rightarrow$ 9/2$^-$ 7000 keV decay of ^{187}Bi^g (cf. Figs. 2 and 3). As discussed above and in Ref. [35], the 9/2$^-$ $\rightarrow$ 9/2$^-$ α decays in the odd-*A* Bi isotopes provide a good example of unhindered decay in this region of nuclei. Therefore, based on the unhindered nature of the 7528 keV α decay we have to assume that it connects two states with the same Nilsson configuration and it is either of the 1/2$^-$ $\rightarrow$1/2$^-$ or 5/2$^-$ $\rightarrow$5/2$^-$ type. That is why we indicated both 1/2$^-$ or 5/2$^-$ as possible I^π values for ^{187}Po and for the 286 keV state in ^{183}Pb in Fig. 2, but most probably the I^π assignments must be the same for both states.

In such a case the strong retardation ($HF_\alpha \geqslant 360$) of the tentatively observed 7808 keV decay to the 3/2$^-$ g.s. in ^{183}Pb is readily understood as due to the large configuration difference involving the decay between the strongly prolate 1/2$^-$ or 5/2$^-$ state in ^{187}Po and the spherical 3/2$^-$ configuration in ^{183}Pb.

To conclude this section, our α-decay data along with the PES/PPR calculations provide unique evidence on the prolate deformation of the 286 keV excited state in ^{183}Pb and of the isotope ^{187}Po.

B. Peculiarities in the α-decay characteristics of the lightest Po isotopes

Figures 5(a) and (b) show the systematics of the α-decay energies and partial α-decay half-lives for isotopes $^{186-202}$Po. Both figures demonstrate that the α-decay energies and partial half-lives of the 3/2$^-$ ground states and of the 13/2$^+$ isomers in the odd-*A* isotopes $^{191-201}$Po follow well the smooth trend of the $0^+_{g.s.} \rightarrow 0^+_{g.s.}$ α decays in their even-*A* neighbors (with the exception of the half-life value of ^{191m}Po, see below). The close resemblance of the α-decay properties of the odd-*A* and even-*A* Po isotopes in this region was interpreted in a simple picture in which the corresponding states in the odd-*A* Po and Pb nuclei are produced by a weak coupling of the valence $3p_{3/2}$ or $1i_{13/2}$ neutron to the nearly spherical even-*A* core. In this approach, the odd neutron is considered as a spectator and is not actively involved in the α-decay process, except for a small correction

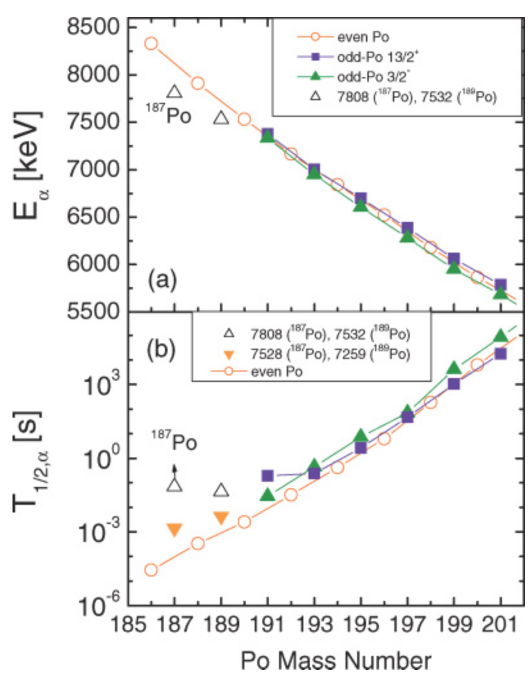

FIG. 5. (Color online) α-decay systematics in Po isotopes: (a) α-decay energies. The largest-energy α decays are shown. For ^{187}Po the energy of the tentatively observed 7808 keV crossover decay is given; (b) Partial $T_{1/2,\alpha}$ values. For ^{187,189}Po the partial half-life values are shown both for the largest-energy (hindered) 7808 and 7532 keV decays and for the strongest (unhindered) fine structure 7528 ^{187}Po, and 7529 keV ^{189}Po decays. The data for ^{186}Po are taken from Ref. [21].

in the α-particle formation probability due to the blocking effect. As discussed in Ref. [9], the occupation of an orbital at the Fermi surface by an odd particle will reduce the α-particle formation probability as it reduces the pairing correlations. Clearly, the blocking effect will have a larger influence in a smaller shell like $3p_{3/2}$ in comparison with a larger one such as $1i_{13/2}$. This is most probably responsible for systematically longer half-lives of the $3/2^-$ g.s. in comparison with the $13/2^+$ states in $^{193-201}$Po. This effect is seen more clearly when discussed in terms of reduced α widths or hindrance factor values, in which the energy dependence is removed from the consideration, see details in Ref. [9]. It is important to note that the weak coupling scheme is also valid for the yrast excited states, see extensive systematics in, e.g., Ref. [4] and references therein.

The α decay of ^{191m}Po ($I^\pi = 13/2^+$) demonstrated a first case of a clear deviation from the smooth behavior in the light odd-A Po isotopes. The striking observation, discussed in detail in Ref. [7], was that although the α-decay energies of ^{191g}Po and ^{191m}Po are different by only 40 keV [Fig. 5(a)], their total half-lives are different by a factor of 4.2, or by a factor of 6.9 if their partial α-decay half-lives are compared, see Fig. 5(b). This phenomenon was interpreted as due to onset of oblate deformation in ^{191m}Po ($I^\pi = 13/2^+$), while the $I^\pi = 3/2^-$ ground state of ^{191}Po continued to be nearly spherical. Thus, the conclusion on shape staggering between two α-decaying isomers in ^{191}Po was drawn [7], which was further confirmed by a dedicated in-beam study of this nucleus [10].

The α decays of ^{189}Po [12] and of the new isotope ^{187}Po (Fig. 2) appear to be even more interesting, as in both cases clear deviations from the systematics are seen both in their α-decay energies and in partial half-life values. For example, Fig. 5(a) shows that the largest-energy α decays of these isotopes (7808 and 7532 keV) are *lower* by $\sim$200 keV (^{189}Po) or by $\sim$300 keV (^{187}Po) relative to the smoothly increasing trend in the even-A Po isotopes. The possibility that this deviation is due to missing α decays of higher energy (by $\sim$200–300 keV) to the ground state is quite unlikely. Indeed, this scenario would require that the 7808 keV decay of ^{187}Po (Fig. 2) and the 7532 keV decay of ^{189}Po [12] feed to excited states at $E^* \sim$ 200–300 keV in ^{183,185}Pb, rather than to their ground states as presently assigned. This, in turn, would require the subsequent deexcitation from these states to the $3/2^-$ ground states. However, no evidence for such transitions as well as for the higher-energy α decays was observed in case of ^{189}Po, for which a larger number of counts was registered in comparison with ^{187}Po. Though due to a lower number of observed decays such a scenario cannot be ruled out completely for ^{187}Po, the similarity of its decay pattern to that of ^{189}Po implies that no higher-energy α-decay branches are present in ^{187}Po as well. Based on the level systematics in the odd-A Pb isotopes, we also discard the possibility that the above-mentioned (hypothetical) excited states are long-lived isomeric states and their decay would not be seen within the time interval of $\Delta T(\alpha - \gamma) \leqslant 5\ \mu$s used in our experiments.

Clearly related to the α-energy irregularities, Fig. 5(b) demonstrates the retarded partial half-lives of the highest-energy 7808 and 7532 keV decays of ^{187,189}Po, which are *longer* than the average of their respective even-A neighbors by a factor of $\sim$40 for ^{189}Po or by a factor of $\sim$500 for ^{187}Po. As shown by the PES calculations in this work and in Refs. [10,12], such a behavior can be interpreted as due to a structure/shape change from the spherical configuration in the heavier $^{193-201}$Po isotopes to a prolate configuration in ^{187,189}Po. The structure/shape changing α decays of ^{187,189}Po toward the spherical g.s. in the Pb isotopes are therefore strongly hindered.

On the other hand, it seems that the fine-structure 7528 keV (^{187}Po) and 7259 keV (^{189}Po) decays, shown by the closed down triangles in Fig. 5(b), follow the same trend as the decay of their even-A neighbors and of the heavier odd-A $^{193-201}$Po isotopes. All these decays proceed between the states of similar structure/shape in parent and daughter nuclei, and therefore are unhindered.

Following the ideas presented in Ref. [39], it is tempting to speculate that the extra binding due to the strong deformation in ^{187,189}Po could then lead to their reduced Q_α-decay energy toward the spherical ground state in the daughter Pb isotopes. However, it is interesting to note that no (or much less) of similar effect is seen in the α-decay energies of the even-A ^{186,188}Po [see Fig. 5(a)], which were interpreted as being of prolate origin as well [11,21]. The latter is probably due to the fact that the shape coexistence occurs at low energy and, therefore, some mixing of different configurations (spherical, oblate, prolate) is expected in the predominantly prolate 0^+ ground states of ^{186,188}Po, which also leads to lower hindrance factor values of HF $\leqslant$ 20 [11,21]. In contrast to this, α decays of ^{187,189}Po proceed from a pure Nilsson single particle state, which results in the above-mentioned peculiarities in their α decay properties and much larger hindrance factors for the decay to the spherical ground state in the Pb isotopes. All above issues will be the subject of a dedicated forthcoming study [40].

V. CONCLUSIONS

By using the complete fusion reaction ^{46}Ti+^{144}Sm $\rightarrow$ ^{187}Po+3n the new neutron-deficient isotope ^{187}Po has been identified at the velocity filter SHIP. Similarly to the earlier studied isotope ^{189}Po, striking features of the ^{187}Po α decay include the strongly-hindered decay to the ground state and unhindered decay to the low-lying deformed excited state at 286 keV in the daughter nucleus ^{183}Pb.

Based on potential energy surface calculations, the ^{187}Po ground state and the observed excited state in ^{183}Pb were interpreted as being of prolate origin. The systematic deviation of the α-decay properties in the lightest odd-A Po isotopes from the smooth behavior in the even-A neighbors is underlined.

Improved α-decay data including more precise half-life values were measured for ^{187}Bi^{m,g}. The excitation energy of ^{187}Bi^m and of the $9/2^-$ and $3/2^+$ excited states in ^{183}Tl were measured with better precision compared to previous studies.

While it is shown that the α-decay method has unparalleled sensitivity in identifying the low-lying excited states in the daughter nuclei, it would be important to perform in-beam studies of ^{183,185}Pb with the aim to find strongly-coupled rotation bands built on top of the prolate intruder bandheads suggested by our studies.

ACKNOWLEDGMENTS

We thank the UNILAC staff for providing the stable and high intensity ^{46}Ti beam. A.N.A. and J.J.R. were partially supported by the NSERC of Canada. This work was supported by the European Commission within the Sixth Framework Programme through I3-EURONS (contract no. RII3-CT-2004-506065), by the FWO-Vlaanderen and by the Interuniversity Attraction Poles Programme - Belgian State - Federal Office for Scientific, Technical and Cultural Affairs (IAP grant P5/07) and UK EPSRC.

[1] F. R. May *et al.*, Phys. Lett. **B68**, 113 (1977).
[2] A. M. Oros *et al.*, Nucl. Phys. **A645**, 107 (1999).
[3] N. A. Smirnova *et al.*, Phys. Lett. **B569**, 151 (2003).
[4] R. Julin, K. Helariutta, and M. Muikku, J. Phys. G: Nucl. Part. Phys. **27**, R109 (2001).
[5] K. Van de Vel *et al.*, Eur. Phys. J. A **17**, 167 (2003).
[6] N. Bijnens *et al.*, Phys. Rev. Lett. **75**, 4571 (1995).
[7] A. N. Andreyev *et al.*, Phys. Rev. Lett. **82**, 1819 (1999).
[8] A. N. Andreyev *et al.*, Nature (London) **405**, 430 (2000).
[9] K. Van de Vel *et al.*, Phys. Rev. C **65**, 064301 (2002).
[10] A. N. Andreyev *et al.*, Phys. Rev. C **66**, 014313 (2002).
[11] K. Van de Vel *et al.*, Phys. Rev. C **68**, 054311 (2003).
[12] A. N. Andreyev *et al.*, Eur. Phys. J. A **6**, 381 (1999); K. Van de Vel *et al.*, *ibid.* **24**, 57 (2005).
[13] D. Wiseman *et al.*, submitted to PRC, in preparation, 2006.
[14] P. Van Duppen and M. Huyse, Hyperfine Interact. **129**, 149 (2000).
[15] M. Huyse *et al.*, Hyperfine Interact. **132**, 141 (2001).
[16] J. O. Rasmussen, Phys. Rev. **113**, 1593 (1959).
[17] H. De Witte *et al.*, to be published (2006).
[18] G. Münzenberg *et al.*, Nucl. Instrum. Methods **161**, 65 (1979).
[19] S. Hofmann *et al.*, Z. Phys. A **291**, 53 (1979); S. Hofmann and G. Münzenberg, Rev. Mod. Phys. **72**, 733 (2000).
[20] A. N. Andreyev *et al.*, Phys. Rev. C **73**, 024317 (2006).
[21] A. N. Andreyev *et al.*, to be published (2006).
[22] S. Saro *et al.*, Nucl. Instrum. Methods A **381**, 520 (1996).
[23] A. N. Andreyev *et al.*, Nucl. Instrum. Methods A **533**, 409 (2004).
[24] F. P. Heßberger *et al.*, Eur. Phys. J. A **22**, 417 (2004).
[25] J. Wauters, P. Dendooven, M. Huyse, G. Reusen, P. Van Duppen, and P. Lievens (ISOLDE Collaboration), Phys. Rev. C **47**, 1447 (1993).
[26] J. C. Batchelder *et al.*, Eur. Phys. J. A **5**, 49 (1999).
[27] A. N. Andreyev *et al.*, Eur. Phys. J. A **18**, 39 (2003).
[28] D. G. Jenkins *et al.*, Phys. Rev. C **66**, 011301(R) (2002).
[29] R. B. Firestone, *Table of Isotopes*, 8th ed. (John Wiley and Sons, Inc., New York, 1996).
[30] P. M. Raddon *et al.*, Phys. Rev. C **70**, 064308 (2004).
[31] A. N. Andreyev *et al.*, Eur. Phys. J. A **18**, 55 (2003).
[32] The program to calculate conversion coefficients. The National Nuclear Data Center (NNDC), http://www.nndc.bnl.gov/nndc/physco/.
[33] A. Hürstel *et al.*, Eur. Phys. J. A **21**, 365 (2004).
[34] H. Kettunen *et al.*, Eur. Phys. J. A **17**, 537 (2003).
[35] A. N. Andreyev *et al.*, Phys. Rev. C **69**, 054308 (2004).
[36] A. N. Andreyev *et al.*, Phys. Rev. C **72**, 014612 (2005).
[37] G. D. Dracoulis, Phys. Rev. C **49**, 3324 (1994).
[38] M. Muikku *et al.*, Phys. Rev. C **64**, 044308 (2001).
[39] R. Fossion *et al.*, Nucl. Phys. **A697**, 703 (2002).
[40] M. Huyse *et al.*, in preparation.